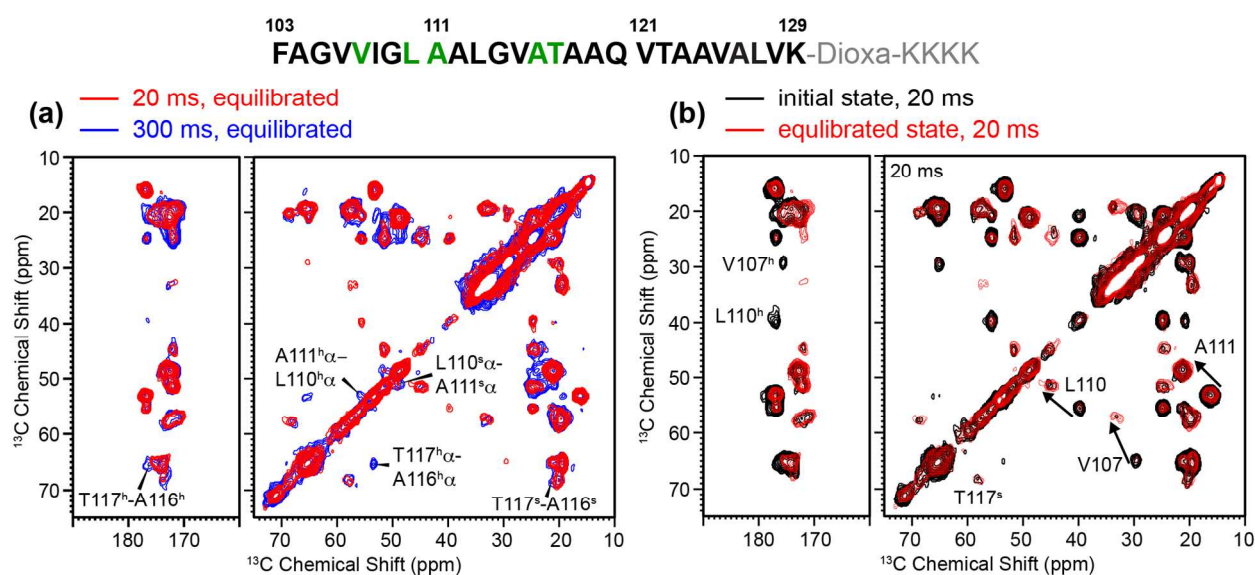


## Support information

# Conformation and Lipid Interaction of the Fusion Peptide of the Paramyxovirus PIV5 in Anionic and Negative-Curvature Membranes From Solid-State NMR

Hongwei Yao and Mei Hong  
Department of Chemistry, Iowa State University, Ames, IA 50011



**Figure S1.** 2D  $^{13}\text{C}$ - $^{13}\text{C}$  correlation spectra of VLAAT-FPK4 in the DOPC/DOPG (4 : 1) membrane in the gel phase. (a) 2D spectra of the equilibrated sample at 20 ms (red) and 300 ms (blue) mixing. Inter-residue cross peaks are observed only for the same secondary structure and not between different secondary structures. For A116 and T117, the  $\alpha$ -helical inter-residue cross peaks are stronger than the  $\beta$ -strand ones, whereas for L110 and A111, the  $\beta$ -strand inter-residue cross peaks are stronger than the  $\alpha$ -helix ones. (b) Overlay of the initial (black) and equilibrated (red) spectra. The initial spectrum shows mainly  $\alpha$ -helical chemical shifts for all labeled residues, while the equilibrated spectrum shows primarily  $\beta$ -strand chemical shifts for N-terminal residues (V107, L110, and A111).

103 111 121 129  
**FAGVVIGL AALGVATAAQ VTAVALVK**-Dioxa-KKKK

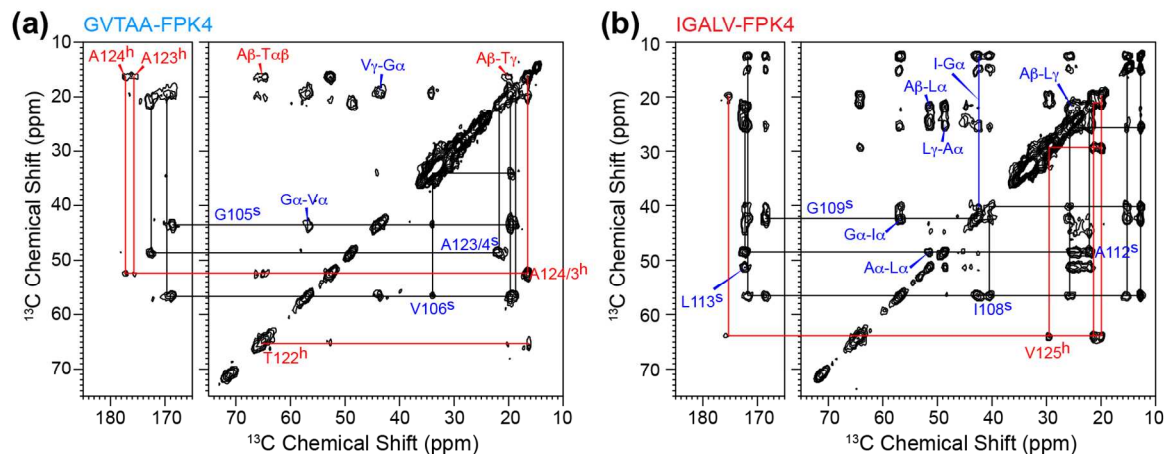


**Figure S2.** 2D  $^{13}\text{C}$ - $^{13}\text{C}$  correlation spectra of FPK4 in the gel-phase DOPC/DOPG (4 : 1) membrane (246 K). (a) GVTAQ-FPK4 spectrum with 500 ms mixing. (b) IGALV-FPK4 spectrum with 500 ms mixing. Inter-residue cross peaks were observed in both spectra, but no cross peak between N-terminal and C-terminal residues is seen. Thus, if the peptide is oligomerized in the DOPC/DOPG bilayer, then the packing is parallel.

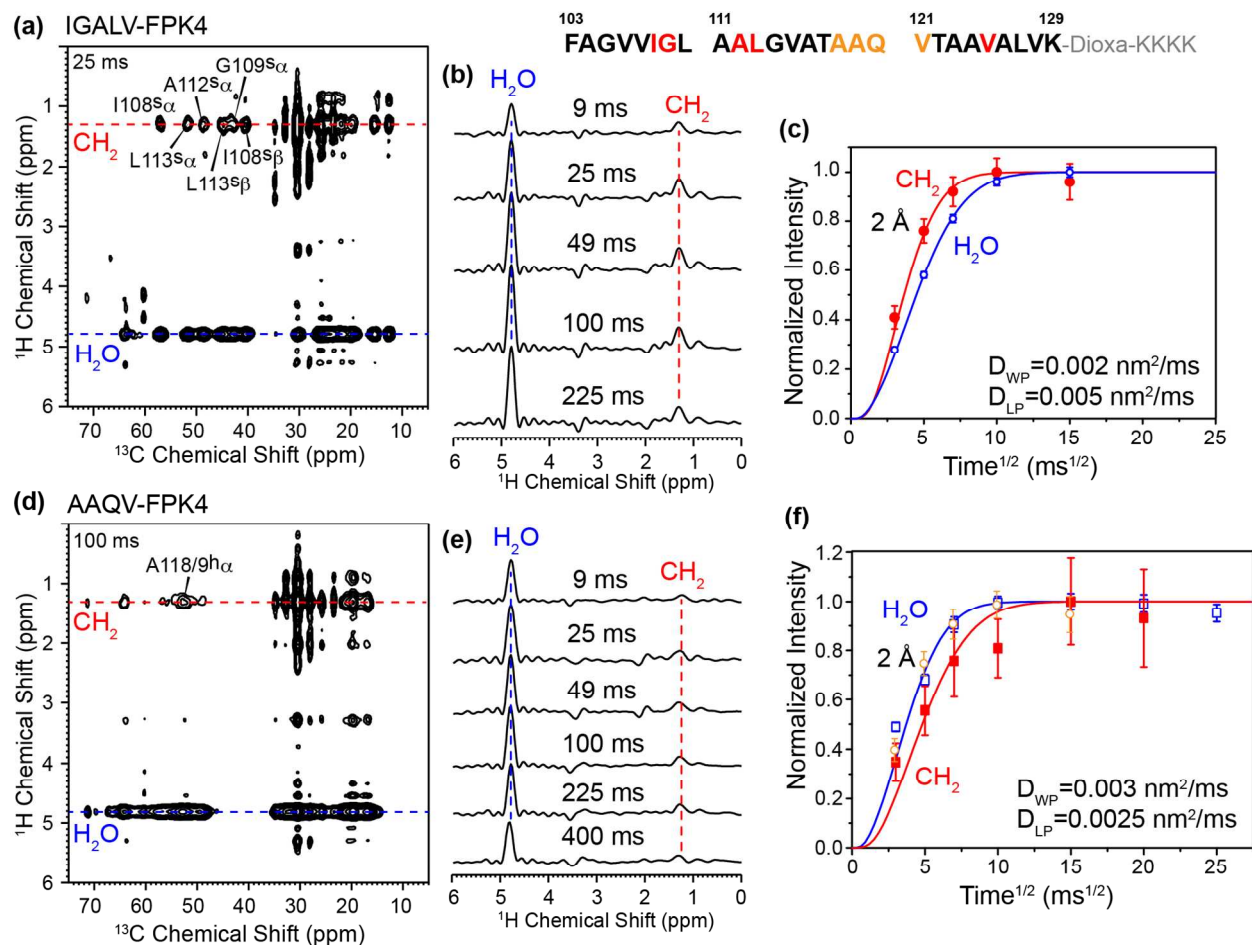


**Fig. S3.** 2D  $^{13}\text{C}$ - $^1\text{H}$  spin-diffusion correlation spectra of FPK4 in the DOPC/DOPG membrane at 293 K. (a) 2D spectrum of IGALV-FPK4 with 25 ms  $^1\text{H}$  spin diffusion. (b)  $^1\text{H}$  cross sections of the 2D spectra with mixing times from 9-225 ms. The cross sections were integrated from  $^{13}\text{C}$  chemical shifts of 37.8-59.0 ppm, corresponding to the  $\beta$ -strand  $\text{C}_\alpha$  and  $\text{C}_\beta$  signals. (c) Measured and best-fit buildup curves of water-peptide (blue) and lipid-peptide (red) spin diffusion. (d) 2D spectrum of AAQV-FPK4 with 100 ms  $^1\text{H}$  spin diffusion. (e)  $^1\text{H}$  cross sections with mixing times of 9-400 ms. The cross sections were integrated from  $^{13}\text{C}$  chemical shifts of 51.5 to 54.0 ppm, corresponding to the  $\alpha$ -helical  $\text{C}_\alpha$  signals. (f) Measured and best-fit buildup curves of water-peptide (blue) and lipid-peptide (red) spin diffusion. Clear lipid-peptide cross peaks are observed for both conformations of the peptide, indicating that FPK4 is well inserted into the DOPC/DOPG membrane.

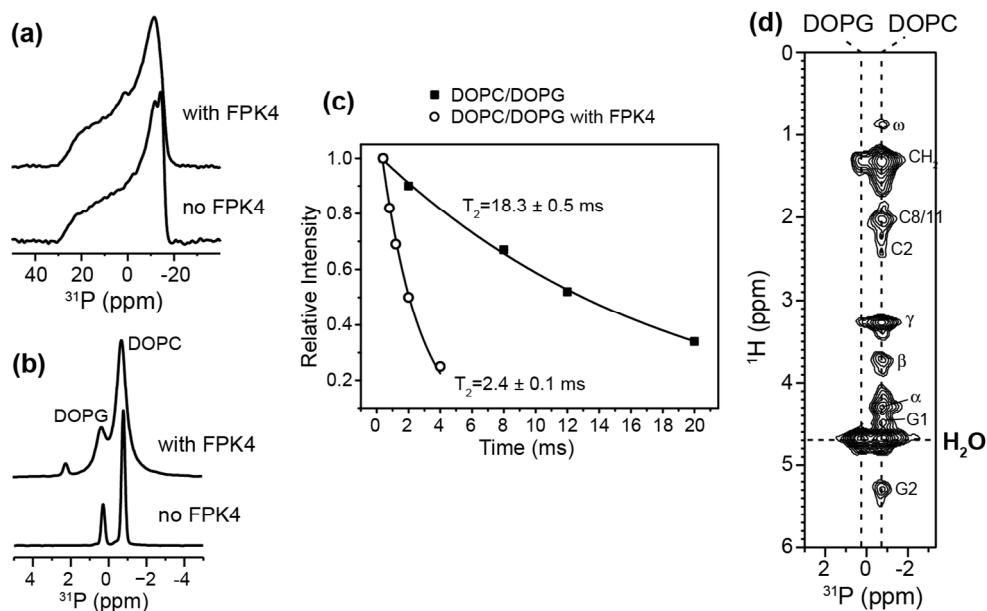


**Fig. S4.** FPK4 interaction with the DOPC/DOPG membrane. (a) 1D  $^{31}\text{P}$  static spectra at 293 K with and without FPK4. (b)  $^{31}\text{P}$  MAS spectra with and without FPK4. The apparent linewidths are  $\sim 30$  Hz for the peptide-free membrane and  $\sim 130$  Hz for the peptide-bound membrane. (c)  $^{31}\text{P}$  transverse relaxation times ( $T_2$ ) of DOPC in the DOPC/DOPG membrane without and with the peptide. The DOPG  $T_2$  values are similar to the DOPC values in the same sample. The  $T_2$  values were measured using a Hahn-echo pulse sequence with a  $^1\text{H}$  decoupling field strength of 50 kHz. (d) 2D  $^{31}\text{P}$ - $^1\text{H}$  correlation spectrum of the peptide-bound sample at 303 K, measured with a  $^1\text{H}$  spin diffusion mixing time of 225 ms.

**Table S1.** Residue-specific helicity (%) of FPK4 in DOPC/DOPG membranes based on the NMR spectral intensities.

Residue	Cross peak	Helicity	Residue	Cross peak	Helicity
G105	C $\alpha$ -CO	0	A116	C $\alpha$ -C $\beta$	54%
V106	C $\alpha$ -C $\beta$	0	T117	CO-C $\alpha$	53%
V107	C $\beta$ -C $\gamma$	34%	A118	C $\alpha$ -C $\beta$	83%
I108	C $\alpha$ -C $\beta$	0	A119	C $\alpha$ -C $\beta$	83%
G109	C $\alpha$ -CO	0	Q120	C $\alpha$ -C $\beta$	100%
L110	C $\alpha$ -C $\beta$	26%	V121	C $\alpha$ -C $\gamma$	85%
A111	C $\alpha$ -C $\beta$	22%	T122	C $\alpha/\beta$ -C $\gamma$	66%
A112	C $\alpha$ -C $\beta$	18%	A123	C $\alpha$ -C $\beta$	57%
L113	C $\alpha$ -CO	17%	A124	C $\alpha$ -C $\beta$	57%
G114	ND	ND	V125	C $\alpha$ -C $\beta$	100%
V115	ND	ND			

For each residue, resolved cross peaks in the 20 ms 2D  $^{13}\text{C}$ - $^{13}\text{C}$  correlation spectra were selected for volume integration. A111 and A116 C $\alpha$ -C $\beta$  cross peaks overlap and indicate a total helical content of 38%. We interpolated the helicities of L110 and A112 to obtain the A111 helicity, and the A116 helicity was the difference between the total helicity and the A111 helicity.